

Asymmetrical Single Cell Multiband Uni-Planar Mushroom Resonant Antenna

Navid Amani and Amir Jafarholi

Institute of Space Science and Technology
Amirkabir University of Technology, 424 Hafez Ave., P.O. Box: 15875-4413, Tehran, Iran
N.Amani@live.com, Jafarholi@ieee.org

Abstract — A new asymmetrical zeroth-order resonant antenna with improved efficiency and widened impedance bandwidth is proposed. It comprises a rectangular patch, two shorted stub and coplanar waveguide (CPW) feed to have composite right/left handed (CRLH) features and easy fabrication process. The asymmetry helps to combine three resonance frequencies and extends the bandwidth up to 31%. The efficiency of the proposed antenna is greater than 94% over the entire bandwidth of 4.2 to 6.2 GHz. The proposed antenna has compact size, which can provide omnidirectional radiation pattern suitable for wireless applications. The proposed antenna has also a low frequency miniaturized resonance at GPS standard 1.57 GHz, while the second frequency band covers 802.11a/h/j/n/ac and 802.11p WLAN, dynamic frequency selection (DFS) and transmit power control (TPC) applications.

Index Terms — Composite right/left-handed transmission line (CRLH TL), multiband antenna, zeroth-order resonant antenna (ZORA).

I. INTRODUCTION

In recent years, introducing metamaterials (MTMs) opened the way for many researcher groups to enhance the antenna performances [1]-[4]. Due to unique electromagnetic properties, MTMs have been widely considered in microstrip antennas to improve their performance; however, the narrow bandwidth of the proposed structures is the main limiting factor for their engineering applications. In addition to these resonance structures, some researchers proposed the other type of MTMs known as composite right/left handed (CRLH) structures which is based on an equivalent circuit approach, [5]. The most famous CRLH resonator is a mushroom structure which employs a patch and via as a unit-cell [6]. Although, periodicity is preferred for computational convenience, applying an element such as unit cell of MTM in antenna structure as a metamaterial-inspired antenna have been proposed and unusual properties of MTM have been achieved [7]-[10]. Based

on CRLH resonator theory, $2N-1$ resonance frequencies are expected from an N -cell mushroom resonator [11]. In the case of one unit-cell, it is expected to have only zeroth-order mode (ZOR); however, the TM_{10} mode of the patch is excited in addition to zeroth-order metamaterial inspired resonance frequency [12]. Although, the TM_{10} mode occurs at a frequency above zeroth-order mode and does not satisfy metamaterial cell size criteria, this is useful especially in one-unit cell mushroom resonator due to dual band operation.

In [8-9] and [12]; the theoretical aspects of CRLH single cell patch antenna is discussed. Here the main focus of the paper is to optimize these designs to have a miniaturized/broadband low-profile antenna. Thus at first the antenna structure is described very briefly, and after that two conventional method to have broadband structure is applied to the proposed antenna, i.e., stepped and tapered structures. In this paper, a new asymmetrical zeroth-order resonant antenna with improved efficiency and widened impedance bandwidth is proposed. It comprises a rectangular patch, two shorted stub and coplanar waveguide (CPW) feed to have CRLH features and easy fabrication process. The asymmetry helps to combine three resonance frequencies and extends the antenna bandwidth. These features are verified by CST Microwave Studio and compared with experimental results.

II. DESIGN PROCEDURE

TL discontinuities are common in microwave circuits and microstrip antennas [13]. T-junction equivalent circuit is nearly similar to CRLH structure. A CRLH unit cell may be achieved just by paralleling the capacitance of the T-junction with the total inductance of the junction and stub, and also introducing a capacitance (C_L) series with RH inductance (L_R). As ground planes are coplanar in CPW, it facilitates easy shunt as well as series. The shunt elements are provided by connecting the stub of the T-junction to CPW ground as a shorted stub. The total inductance of the junction and stub becomes parallel with the total capacitance of the structure.

In addition, the gap existence between CPW central strip and main line of the T-junction introduces a LH capacitance C_L . Three different configuration of a single cell uni-planar mushroom CRLH resonant antenna based on T-junction discontinuity and ungrounded CPW feed are realized. In the case of one unit cell there is neither left-hand capacitance nor negative-order modes. Nonetheless, zeroth-order and TM_{10} modes are achievable and dual-band operation is applicable. Asymmetrical configuration provides another resonance frequency below both the zeroth-order and TM_{10} modes; therefore, tri-band functionality is provided. We consider step and linear taper in the main line of the T-junction to combine zeroth-order and TM_{10} modes and enhance the antenna bandwidth.

A. Zeros order mode

Zeroth-order resonance frequency can be achieved by the following:

$$\omega_{sh} = \frac{1}{\sqrt{L_L C_R}}, \quad (1)$$

where L_L and C_R are the left-hand inductance and right-hand capacitance, respectively. The right-hand capacitance is achieved through the gap between the rectangular strip and CPW ground planes. Left-hand inductance which is introduced by the means of shorted stub is determined by the width and length of the stub. These are influential parameters in ZOR frequency.

B. Positive- and negative-order modes

In contrast to zeroth-order mode, both positive- and negative-order modes are affected by the cells number, [11]. Simulations show that the number of resonance frequencies for these right- and left-handed regions are dependent on the number of cells, cell types and feeding configuration.

In general, CRLH structure is a band-pass filter due to the lowpass nature of the right-handed (RH) elements and the highpass nature of the LH elements. In a periodic CRLH TL net rejection commonly occurs from the structure, due to satisfaction of Bragg condition at both ends of the Brillouin zone. In a periodic CRLH resonator, the resonance frequencies obtained by [11]:

$$\beta_n p = \frac{n\pi}{N} (n = 0, \pm 1, \dots, \pm N), \quad (2)$$

where n is the mode number and N is the number of unit cells. Therefore, $2N+1$ resonances (i.e., N RH, N LH and one as zeroth-order mode) may be achieved in a CRLH resonator. When $|n|=N$, the dispersion diagram reaches to the edges of Brillouin zone where the period of the structure is equal to $|\lambda/2|$. Thus, there is a potential to

satisfy Bragg condition with in-phase reflections from unit cells with sizes of $|\lambda/2|$. In this condition no energy transmits to the structure and consequently the corresponding resonances, known as Bragg frequencies, are eliminated. Generally, there are two Bragg frequencies in a multi-cell CRLH resonator, a resonance occurred in RH region and the other is located in LH region. Therefore, $2N-1$ resonance frequencies may be obtained. By reducing the number of cells, in-phase reflections from the adjacent cells will become progressively weaker. Eventually, in a single-cell CRLH resonator due to periodicity elimination, there is not any in-phase reflection from the adjacent cells and it causes to disappear Bragg gaps, which is consequently leads to obtain two additional resonance frequencies. It is worth nothing that the amount of bandgap decreasing at the RH region is greater than LH which is due to harmonic nature of the structure.

Simulation shows that this condition is much sensitive and strongly dependent to cell-types and feeding structure. As a result, a single-cell CRLH resonant antenna performs tri-band characteristic while occupying less area than a multi-cell CRLH resonant antennas and further miniaturization is achievable without missing multiband functionality.

In [9] it is shown that the ZOR frequency which is derived from dispersion diagram is equal for a single-cell and multi-cells CRLH resonators. Although zeroth-order resonance frequency in an open-ended CRLH resonator is independent of the series elements, any changes in shunt elements will shift all negative-, zeroth- and positive-order resonance frequencies. The width and location of the stub have determinative role in resonance frequencies, due to changes in shunt capacitance/ inductance values.

III. ANTENNA REALIZATION

A. Simple T-antenna

To have preferable impedance matching condition, a 50Ω input impedance ungrounded CPW line is designed. The widths of the main line and central strip of the CPW have major effect on antenna matching. In order to achieve more coupling and better matching condition, the central strip of the CPW is designed wider at the end of the line ($W_2 > W_1$). To realize shunt elements, the stub of the junction is connected to the CPW ground plane. Shorted stub and gap dimensions between main line of the T-junction and CPW ground plane determine shunt parameter values and ZOR frequency of the structure. The schematic of the proposed CRLH resonant simple T-antenna and the manufactured prototype are shown in Fig. 1 (a).

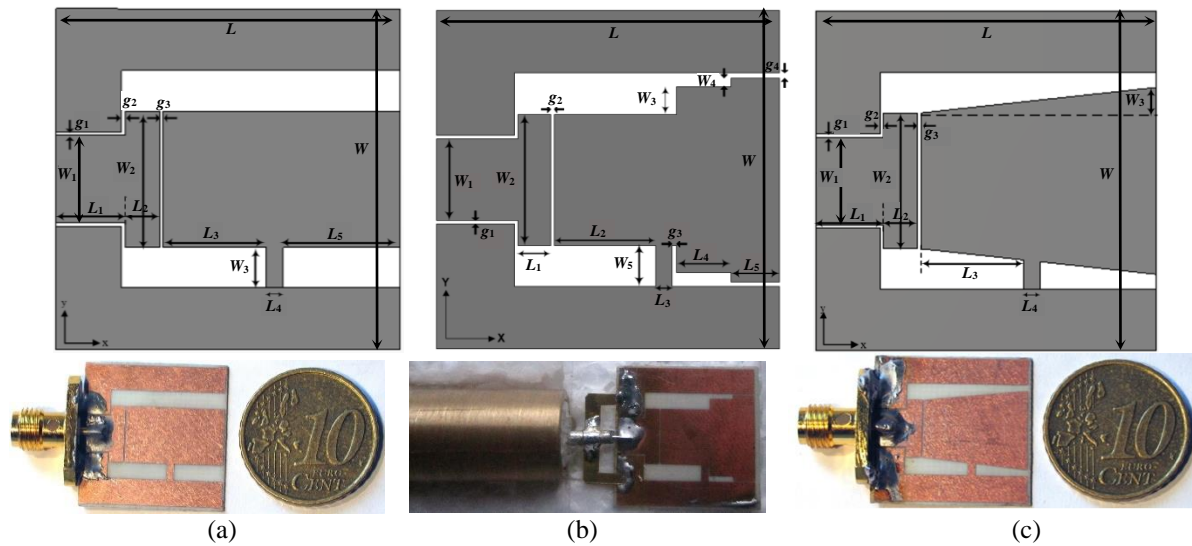


Fig. 1. Schematic of the proposed single-cell: (a) simple, (b) step tapered, and (c) linear tapered T-shape CRLH resonant antenna based on the T-junction discontinuity and CPW feed structure. Photograph of the manufactured prototype. All dimensions are (in mm): $W=L=20$, $W_1=5.15$, $W_2=8$, $g_1=g_2=g_4=0.2$, $W_4=0.6$, $W_5=2.375$; for simple type antenna: $W_3=2.375$, $L_1=4$, $L_2=2$, $L_3=6$, $L_4=1$, $L_5=6.8$, $g_3=0.2$; for step tapered T-antenna: $W_3=1.575$, $L_1=2$, $L_2=6$, $L_3=1$, $L_4=3.42$, $L_5=3.16$, $g_3=0.22$, for linear tapered antenna: $W_3=1$.

To show the effects of the shorted stub and the CRLH characteristics of the proposed structure, simulated impedance diagram of the simple T-antenna is compared with a CPW-fed simple patch without shorted stub (Fig. 2). According to this figure, the fundamental resonance frequency of a simple rectangular patch antenna is obtained around 5.8 GHz, while the proposed simple T-antenna has a little shift to upper frequencies at this mode and provides two additional resonances below this TM_{10} mode. Figure 3 demonstrates the simulated and measured reflection coefficient of the proposed T-antenna. However, zeroth-order mode of the proposed antenna is obtained at approximately 4.22 GHz. The measured asymmetry and TM_{10} modes occurred at 1.72 and 5.8 GHz, respectively. At the asymmetry mode the overall antenna dimensions is $20\text{mm}\times 20\text{mm}\times 0.508\text{mm}$ ($0.11\lambda\times 0.11\lambda\times 0.003\lambda$). The measured -10 dB bandwidth at asymmetry, zeroth-order and TM_{10} modes are 3.08%, 15.17% and 8.33%, respectively. In order to delineate the tri-band functionality of the proposed structure, the tangential electric field distribution of the proposed simple T-antenna at asymmetry, zeroth-order and TM_{10} modes are depicted in Fig. 4. It seems that there is a strong coupling between CPW feed and the radiating T-shape patch at all three modes that preserves the efficiency of the antenna. Owing to asymmetry of the patch, asymmetrical electric field distribution in CPW feed region are clearly observed at both asymmetry and zeroth-order modes while it is more symmetrical in TM_{10} mode.

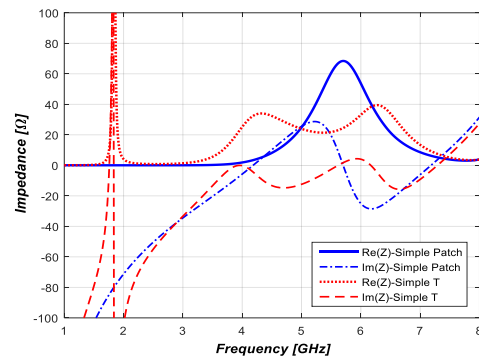


Fig. 2. Comparison of input impedance of the proposed single-cell CRLH resonant T-antenna with the simple rectangular patch without shorted stub.

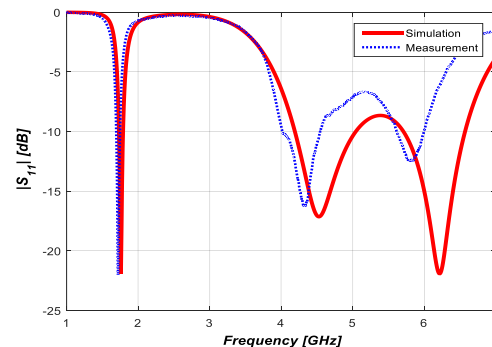


Fig. 3. Simulated and measured reflection coefficients of the proposed single-cell CRLH resonant T-antenna.

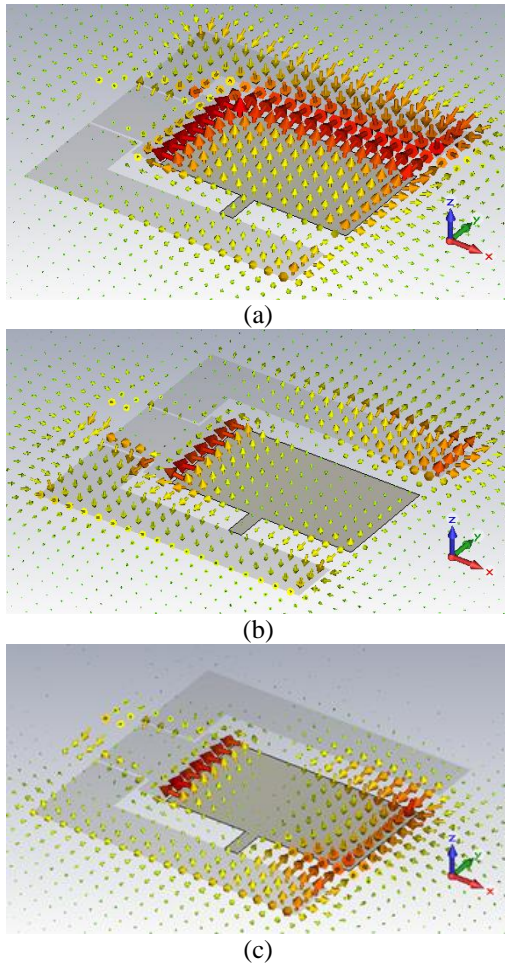


Fig. 4. Electric-field distribution of the simple T-antenna: (a) $n=-1$ mode, (b) $n=0$ mode, (c) $n=+1$ mode; asymmetrical electric field distribution in CPW feed region at both $n=-1, 0$ modes and symmetrical electric field distribution in $n=+1$.

B. Step tapered T-antenna

Accordant to impedance diagram of the simple T-antenna, Fig. 2, there is a great potential to combine zeroth-order and TM_{10} modes with small changes in the original structure. One common way to improve matching condition is to use reactive elements. It is well-known that microwave discontinuities can introduce reactive elements. Multiple step discontinuities with different length and width, generally used to improve impedance matching [14]. The schematic of the proposed step tapered single-cell uniplanar mushroom resonant antenna and its manufactured prototype are shown in Fig. 1 (b). The return loss diagram of the proposed antenna is shown in Fig. 5. Here, the miniaturization band or asymmetry mode reduced to 1.57 GHz. At this frequency, the antenna dimension is approximately $0.1\lambda \times 0.1\lambda \times 0.0026$, while the measured bandwidth is about 31.4 MHz.

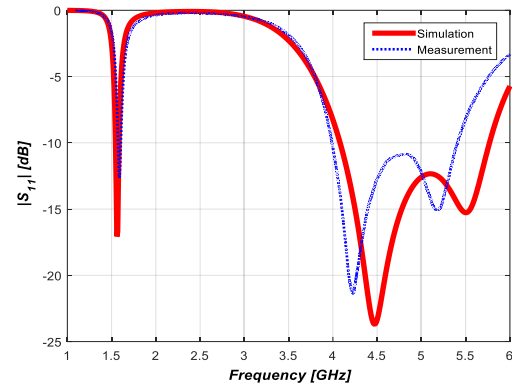


Fig. 5. Simulated and measured reflection coefficients of the single-cell step tapered CRLH resonant T-antenna.

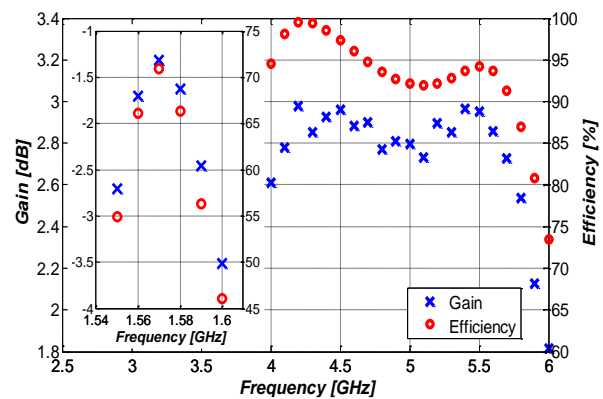


Fig. 6. Measured gain and simulated efficiency of the single-cell step tapered CRLH resonant T-antenna: (a) miniaturized lower, and (b) higher frequencies.

With the aid of two step discontinuities zeroth-order and TM_{10} modes became closer together and combined with significant 30.8% measured impedance bandwidth. The proposed antenna has -1.3 dB gain and considerable 70.8% total efficiency in miniaturization band due to integrated structure. Antenna dimension in the middle of its upper band is $0.3\lambda \times 0.3\lambda \times 0.0077$ with increased efficiency and extended bandwidth. The measured gain and simulated efficiency of the proposed antenna are plotted in Fig. 6.

The CST-predicted and measured far-field radiation patterns of the proposed tri-band single-cell uniplanar mushroom resonant antenna are also shown in Fig. 7 at $f=1.5$ and 4.2 GHz. To measure the antenna radiation pattern, the sleeve balun is used which is designed and fabricated to measure the radiation at a single resonance frequency due to its narrowband behavior [9]. For the sake of brevity we omit the results, however for all three types of proposed antenna the measurements have done using sleeve balun as described and depicted here. As expected, the results show that the proposed antenna has fairly good omnidirectional radiation patterns at the XZ-

plane ($\varphi=0$) and YZ-plane ($\varphi=90$).

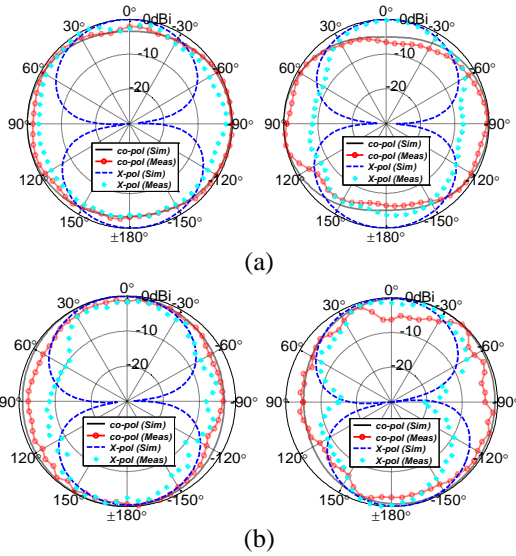


Fig. 7. Comparison of CST-predicted and measured radiation patterns, XZ-Plane (left) and YZ-Plane (right), for dualband step tapered CRLH resonant T-antenna: (a) 1.5 GHz and (b) 4.2 GHz.

Because the size of the proposed antenna in the highest resonance frequency is less than 0.5λ (about 0.38λ), omnidirectionality of radiation patterns is preserved in the entire impedance bandwidth at all three modes.

According to the applications of the proposed miniaturized tri-band antenna in mobile communication systems, the level of cross-polarized radiation pattern is not critical.

C. Linear tapered T-antenna

Continuous step discontinuities with differential length and width extension transform to tapered line. The

schematic of the proposed linear tapered CRLH resonant antenna and the manufactured prototype are shown in Fig. 1 (c). The zeroth-order mode shifted up to 4.5 GHz. Reflection coefficient diagram of the proposed linear tapered T-antenna shows better impedance matching in the frequency range between zeroth-order and TM_{10} modes, Fig. 8, and in upper band, remarkable 37.97%, for -10 dB measured impedance bandwidth is achieved. The measured antenna bandwidth at the miniaturized frequency is about 44 MHz where the antenna dimension is $0.11\lambda \times 0.11\lambda \times 0.003\lambda$.

Table 1 shows the overall performance of the proposed step tapered T-antenna in comparison with the recently reported ZOR antennas [15], [16], [17], [18]. Deficiencies of the reference antennas are highlighted in the table. In [15] and [16] two and three unit cells are used, respectively while dipole-like pattern is achieved. The proposed single-cell ZOR antenna in [17] suffers from narrow bandwidth. Although, another single-cell ZOR antenna is presented in [18], the proposed antenna becomes 3-dimensional and bulky due to folded mushroom structure.

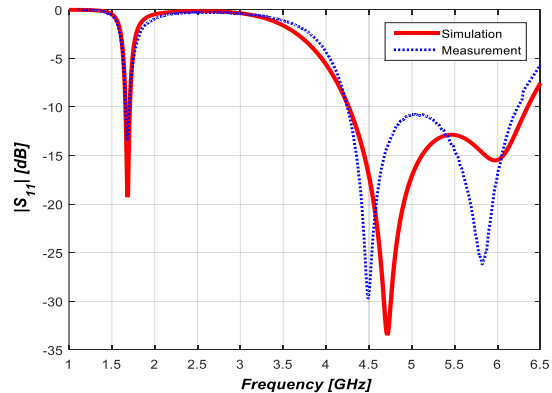


Fig. 8. Simulated and measured reflection coefficients of the single-cell linear tapered CRLH resonant T-antenna.

Table 1: Summary of antenna performances for the proposed and reference antennas

Frequency (GHz)	Step Tapered T-Antenna		[15]	[16]	[17]	[18]
	Lower band (1.57)	Upper band 4.2-6.2 ($f_c=4.59$)	2.03	2.78	2.67	3.58
Antenna footprint (λ_0)	$0.1 \times 0.1 \times 0.0026$	$0.3 \times 0.3 \times 0.007$	$0.17 \times 0.14 \times 0.01$	$0.46 \times 0.24 \times 0.01$	$0.22 \times 0.33 \times$	$0.36 \times 0.23 \times 0.18$
Number of cells	1		2	3	1	1
Antenna type	Miniaturized	Low profile	Low profile	Low profile	Low profile	3-Dimensional
Bandwidth (%)	2	30.8	6.8	70.5	0.6	68.3
Efficiency (%)	70.8	94	62	82	-	>80
Gain (dB)	-0.59	2.9	1.35	2	1.22	>3
Pattern type	Omnidirectional	Omnidirectional	Dipole-like	Dipole-like	Omnidirectional	Omnidirectional

IV. CONCLUSION

A new asymmetrical uni-planar resonant antenna which comprises of simple patch, shorted rectangular

strip and ungrounded CPW feed has been proposed. Using step and linear tapered structures, a dual-band antenna which has a miniaturized lower-band resonance

frequency, at GPS standard 1.57 GHz, as well as wideband upper-band frequencies, from 4.2 to 6.2 GHz, have been proposed. The effects of unit cell number on the zeroth-order bandgap and the number of resonance frequencies in a CRLH resonator is illustrated here. It is shown that reducing the number of cells does not have considerable effects on the zeroth-order mode. In the other word, to design a miniaturized single-cell CRLH resonant antenna, someone may assume a periodic boundary condition, in order to extract the relative dispersion diagram and zeroth-order resonance frequency. To address simultaneously a compact multiband CRLH resonant antenna with high efficiency, a single-cell T-junction based CPW-fed antenna is proposed. In contrast to other ZORAs, a good impedance matching in all resonances is achieved while the antenna efficiency is high. The proposed antenna is implemented on a single layer thin substrate without via process resulting in a simple fabrication. Based on mentioned theoretical concepts, two types of proposed structure have been utilized, i.e., tri-band and dual-band CRLH resonant antennas.

REFERENCES

- [1] L. Liu, C. Caloz, and T. Itoh, "Dominant mode leaky-wave antenna with backfire-to-endfire scanning capability," *Electron. Lett.*, vol. 38, no. 23, pp. 1414-1416, Nov. 2002.
- [2] M. Rafaei Booket, M. Veysi, Z. Atlasbaf, and A. Jafarholi, "Ungrounded composite right/left handed metamaterials: Design, synthesis, and applications," *IET Microwave Antenna Propag.*, vol. 6, no. 11, pp. 1259-1268, 2012.
- [3] A. Jafarholi and M. H. Mazaheri, "Broadband microstrip antenna using epsilon near zero metamaterials," *IET Microwave Antenna Propag.*, accepted, 2015.
- [4] A. Jafarholi, M. Kamyab, and M. Veysi, "Artificial magnetic conductor loaded monopole antenna," *IEEE Antennas Wireless Propag. Lett.*, vol. 9, pp. 211-214, 2010.
- [5] A. Sanada, C. Caloz, and T. Itoh, "Novel zeroth-order resonance in composite right/left-handed transmission line resonators," *Proc. Asia-Pacific Microw. Conf.*, vol. 3, pp. 1588-1591, 2003.
- [6] D. Sievenpiper, L. Zhang, R. F. J. Broas, N. G. Alexopolous, and E. Yablonovitch, "High-impedance electromagnetic surfaces with a forbidden frequency band," *IEEE Trans. Antennas Propag.*, vol. 47, no. 11, pp. 2059-2074, Nov. 1999.
- [7] A. Erentok and R. W. Ziolkowski, "Metamaterial-inspired efficient electrically small antennas," *IEEE Trans. Antennas Propag.*, vol. 56, no. 3, pp. 691-707, 2008.
- [8] N. Amani, A. Jafarholi, M. Kamyab, and A. Vaziri, "Asymmetrical wideband zeroth-order resonant antenna," *Electron. Lett.*, vol. 50, no. 2, pp. 59-60, 2014.
- [9] N. Amani, M. Kamyab, A. Jafarholi, A. Hosseinbeig, and J. S. Meiguni, "Compact tri-band metamaterial-inspired antenna based on CRLH resonant structures," *Electron. Lett.*, vol. 50, no. 12, pp. 847-848, 2014.
- [10] M. Rafaei Booket, A. Jafarholi, M. Kamyab, H. Eskandari, M. Veysi, and S. M. Mousavi, "Compact multi-band printed dipole antenna loaded with single-cell metamaterial," *IET Microw. Antennas Propag.*, vol. 6, pp. 17-23, 2012.
- [11] C. Caloz and T. Itoh, *Electromagnetic Metamaterials: Transmission Line Theory and Microwave Applications*. New York: Wiley, 2006.
- [12] N. Amani, M. Kamyab, and A. Jafarholi, "Zeroth-order and TM_{10} modes in one-unit cell CRLH mushroom resonator," *IEEE Antennas Wireless Propag. Lett.*, vol. 14, pp. 1396-1399, 2015.
- [13] K. C. Gupta, R. Garg, I. Bahl, and P. Bhartia, *Microstrip Lines and Slotlines*. 2nd ed., Artech House, 1996.
- [14] G. V. Eleftheriades, A. K. Iyer, and P. C. Kremer, "Planar negative refractive index media using periodically L-C loaded transmission lines," *IEEE Trans. Microw. Theory Tech.*, vol. 50, no. 12, pp. 2702-2712, Dec. 2002.
- [15] T. Jang, J. Choi, and S. Lim, "Compact coplanar waveguide (CPW)-fed zeroth-order resonant antennas with extended bandwidth and high efficiency on vialess single layer," *IEEE Trans. Antennas Propag.*, vol. 59, no. 2, pp. 363-372, 2011.
- [16] B. Niu and Q. Feng, "Bandwidth enhancement of CPW-fed antenna based on epsilon negative zeroth- and first-order resonators," *IEEE Antenna Wireless Propag. Lett.*, vol. 12, pp. 1125-1128, 2013.
- [17] T. G. Kim and B. Lee, "Metamaterial-based compact zeroth-order resonant antenna," *Electronics Letters*, vol. 45, no. 1, pp. 12-13, Jan. 2009.
- [18] S. Ko and J. Lee, "Wideband folded mushroom zeroth-order resonance antenna," *IET Microw. Antennas Propag.*, vol. 7, pp. 79-84, 2013.